Hindawi
Journal of Food Biochemistry
Volume 2023, Article ID 4174625, 12 pages
https://doi.org/10.1155/2023/4174625

Research Article

UPLC-Q-Exactive-MS Combined with Network Pharmacology to Explore the Antitumor Effect of *Polygonatum sibiricum* Leaf Tea

Jie Chen,[1] Jie Xia,[2] Feng Yin,[2] Jiani Yu,[2] Jinfeng Huo,[3] Yingjiao Shi,[3] Ruilian Han,[1] Zhongda Zeng,[3] and Xiaodan Zhang[2]

[1]*School of Architectural Engineering, Zhejiang Sci-Tech University, Hangzhou, China*
[2]*Key Laboratory of Plant Secondary Metabolism and Regulation of Zhejiang Province, College of Life Sciences and Medicine, Zhejiang Sci-Tech University, Hangzhou, China*
[3]*College of Environmental and Chemical Engineering, Dalian University, Dalian, China*

Correspondence should be addressed to Zhongda Zeng; zeng@chemdatasolution.com and Xiaodan Zhang; zhangxiaodanzstu@163.com

Received 10 April 2023; Revised 12 November 2023; Accepted 30 November 2023; Published 15 December 2023

Academic Editor: Rafik Balti

Background. Currently, the substance basis and function of *Polygonatum sibiricum* leaf remain unknown. *Objective*. This study aims to investigate the antitumor mechanism of *P. sibiricum* leaf tea through network pharmacology. *Methods*. Ultraperformance liquid chromatography quadrupole exactive mass spectrometry (UPLC-Q-Exactive-MS) was employed to analyze the chemical components in the extract of *P. sibiricum* leaf tea. Compounds were screened using the PubChem database and SwissADME platform. The compound targets were identified using the Swiss Target Prediction database, while the disease targets were obtained from the GeneCards database. Subsequently, a compound-protein interaction network was constructed, and KEGG pathway enrichment analysis was performed to elucidate the antitumor activity pathway of *P. sibiricum* leaf tea. Molecular docking verification was carried out as well. *Results*. From the extract of *P. sibiricum* leaf tea, a total of fifty-six components were screened, including 27 active components. Seventy-two corresponding targets closely associated with the antitumor activity of *P. sibiricum* leaf tea were identified. By constructing a compound-target-pathway network diagram, three key compounds (pubescenol, avenanthramide E, and 13-cis-acitretin) and eleven key targets (AKT1, EGFR, CASP3, CCND1, MTOR, MMP9, ERBB2, BCL2L1, MAPK1, PPARG, and PIK3CA) were determined. Additionally, KEGG pathway analysis identified 30 antitumor related pathways. The results of molecular docking between the three key compounds and the top three targets (AKT1, EGFR, and CASP3) were consistent with the findings of network pharmacology. *Conclusion*. This study highlights the distinctive features of *P. sibiricum* leaf tea extract, which possesses multiple components, targets, and pathways. It successfully identifies the active components of *P. sibiricum* leaf tea that exhibit antitumor properties, along with their potential mechanisms of action. These findings offer valuable insights and inspiration for further research on novel mechanisms of action.

1. Introduction

Chinese Pharmacopoeia explains that Polygonatum includes *Polygonatum sibiricum* Red., *Polygonatum kingianum* Coll. et Hemsl., and *Polygonatum Cyrtonema* Hua. *Polygonatum sibiricum* is a perennial herb of Polygonatum in Liliaceae. Pharmacological studies have found that Polygonati Rhizoma has the functions of reducing blood sugar [1], antitumor [2], anti-inflammatory [3], and so on. Although Polygonatum is the same source of medicine and food and its roots, leaves, flowers, and fruits can be eaten as recorded in Chinese Traditional Medical Books [4], however, modern studies mainly focus on the genetic diversity of *P. sibiricum* plants [5], transcriptome analysis of *P. sibiricum* rhizome [6], development of molecular marker technology [7], and biological activity of *P. sibiricum* polysaccharide [8], while there have been few studies on *P. sibiricum* leaves. It has been shown in the literature that *P. sibiricum* leaves contain a variety of flavonoids and phenolic acids, which have certain lipase inhibitor activities. In vitro activity experiment results show that the extract of *P. sibiricum* leaves may have lipid-lowering effects [9], but its material basis and biological effects are still unclear. From the aspect of high-value utilization of *P. sibiricum* leaf, the research and development of *P. sibiricum* leaf is the general trend. Therefore, in this study, we aim to comprehensively investigate the unused part of *P. sibiricum*, the leaves of *P. sibiricum*, and make it into tea so as to increase its use and reduce waste.

The data of GLOBOCAN 2018 [10] show that the mortality rate of cancer is very high in China, and malignant tumor is often one of the causes of cancer. In the past few years, clinical drug problems such as tumor resistance have emerged, patients have experienced adverse reactions after surgery [11], people have gradually turned to the development of innovative anticancer drugs [12], especially now, and more and more traditional Chinese medicine has been proved to have good antitumor effects [13–15]. Therefore, screening the Chinese medicines and compounds with potential antitumor drug development potential has become a research hotspot in recent years.

The LC-MS/MS technology has been widely used in the identification of effective components of traditional Chinese medicine [16, 17]. Among them, the ultraperformance liquid chromatography quadrupole exactive mass spectrometry (UPLC-Q-Exactive-MS) has the characteristics of high resolution, quality accuracy, and quality range, which can quickly identify the components [18]. Ren et al. [19] compared the type and content of metabolites in rats based on this technique and identified the metabolic pathway of alkaloids. In addition, Liu et al. [20] applied this technology to the food field to identify changes in metabolites of beef secretion. Li et al. [21] also used this technique to compare metabolome of Yigong tea at different harvesting periods. Therefore, we aim to use UPLC-Q-Exactive-MS technology to determine the chemical composition of the *P. sibiricum* leaf tea.

Network pharmacology is an important tool for the research of system bioinformatics. It uses the network visualization method to analyze the complex interaction relationship among diseases, drugs, and targets, which has the characteristics of integrity and systematicness. It has been widely used to predict the mechanism of regulation of biological networks by traditional Chinese medicine [22–24]. For example, network pharmacology has been applied in the study on the mechanism of TCM treatment of ulcerative colitis [25]. Peng et al. [26] also used network pharmacology to study diosgenin inhibiting prostate cancer by inducing UHRF1 protein degradation. Xiong et al. [27] studied the antidepressant mechanism of *Angelica dahurica* based on its active components. Therefore, in this study, we combined network pharmacology to clarify the antitumor mechanism of *P. sibiricum* leaf tea.

In this study, UPLC-Q-Exactive-MS was used to conduct rapid qualitative analysis of the chemical components of *P. sibiricum* leaf tea, and the efficacy of the antitumor effect of *P. sibiricum* leaf tea and the material basis of the molecular mechanism were discussed in combination with network pharmacology so as to provide a scientific basis for the further development of *P. sibiricum* leaves.

2. Materials and Methods

2.1. Drugs and Reagents. Polygonatum sibiricum leaf tea, from Jiuxian Mountain, Wulian County, Rizhao City, Shandong Province, China. It was identified by Professor Chen Haimin of Zhejiang Sci-Tech University and stored in the laboratory of School of Life Science and Medicine of Zhejiang Sci-Tech University with the sample number HJY-1. Chromatographically, pure methanol and acetonitrile were purchased from Merck, Germany. The high-purity water comes from the ultrapure water machine of the American Millipore Laboratory. Formic acid and ammonium bicarbonate were purchased from Sigma Company in the United States.

2.2. Instrument. Q-Exactive high resolution mass spectrometry system (Thermo, USA), equipped with Ultimate 30000 UPLC ultrahigh performance liquid phase system (Thermo, USA); and Xcalibur data acquisition software (Thermo, USA). Centrifuge 5417R (Eppendorf, Germany); Vortex Mixer T1 vortex oscillator (Titan SCIENTIFIC LAB); TIMI-10K micro centrifuge (Titan SCIENTIFIC LAB); Labconco centrifugal concentrator (Labconco, American).

2.3. Database and Software. The structure of the compounds from the PubChem database (https://pubchem.ncbi.nlm.nih.gov/) is given. SwissADME platform (https://www.swissadme.ch/) to screen the active compounds by Swiss Target Prediction platform (https://www.swisstargetprediction.ch/) to predict targets. Drug targets are imported into the UniProt (https://www.uniprot.org/) database; input the name of the target gene to define the species as "Homo sapiens" and standardize. Search GeneCards (https://www. genecards.org) to obtain the antitumor active ingredients and corresponding targets of *P. sibiricum* leaf tea and target the tumor and related diseases. The protein interaction network was obtained using the STRING database (https://cn.string-db.org/) combined with Cytoscape v3.7.2 software. Use DAVID (https://david.ncifcrf.gov/) to KEGG pathway analysis (https://www.kegg.jp/). The structure of the compound was obtained from PubChem database; the structure of the target is obtained from the PDB database (https://www.pdb.org); the docking simulation was performed using Auto Dock 4.2 software.

2.4. Composition Analysis of P. sibiricum Leaf Tea

2.4.1. Sample Solution Preparation. Operate on ice, accurately weigh 100 mg of plant sample into 2 mL QSP tube, and record its weight. Join 400 μL cold methanol (including internal standard), vortex oscillation for 1 min. Add 2 steel balls at 4°C. Grind at 50 Hz frequency for 4 min and take out the steel ball. Then, the ultrasonic probe is used for extraction to make it fully extracted. Vortex oscillates for 1 min and stands at low temperature for 10 min. Centrifuge at 14000 g speed at 4°C for 15 min. Suck the supernatant 200 μL and put it in a new EP tube, centrifuge at low temperature and concentrate it and then store it in a −20°C refrigerator for standby. Before the machine analysis, the metabolite extract solution sample was redissolved with 100 μL 20% methanol/water solution, and then the supernatant was taken by centrifugation until completely dissolved, and the positive and negative ion mode analysis was carried out.

2.4.2. Chromatographic (UPLC) Conditions. Positive ion mode: chromatographic column: BEH C8 column, 1.7 μm, 2.1×100 mm (Waters, USA); column temperature: 50°C; injection volume: 10 μL; mobile phase A: water (containing 0.1% formic acid); mobile phase B: acetonitrile (containing 0.1% formic acid); flow rate: 0.35 mL/min; gradient elution procedure: 5% phase B is the initial concentration, 0-1 min, phase B is kept at 5%, 1–24 min, phase B changes from 5% to 100%, 24.1–27.5 min, phase B is kept at 100%, 27.6 min–30 min, and phase B is kept at 5%.

Negative ion mode: chromatographic column: HSS T3 column, 1.8 μm, 2.1×100 mm (Waters, USA); column temperature: 50°C; injection volume: 10 μL; mobile phase A: water (containing 6.5 mM ammonium bicarbonate); mobile phase B: 95% methanol water (containing 6.5 mM ammonium bicarbonate); flow rate: 0.35 mL/min; gradient elution procedure: 5% phase B is the initial concentration, 0 min-1 min, phase B is kept at 5%, 1–18 min, phase B changes from 5% to 100%, 18.1–22 min, phase B is kept at 100%, 22.1–25 min, and phase B is kept at 5%.

2.4.3. Mass Spectrometry (MS) Conditions. The heated electric spray ion source HESI positive and HESI negative modes are adopted, and the primary full scan + DDA secondary subion scan mode is adopted. Spray voltage (kV) is +3.8, and spray voltage (kV) is −3.0. Capillary temperature (°C): 320; aux gas heater temperature (°C): 350; sheath gas flow rate (Arb): 35; aux gas flow rate (Arb): 8; S-lens RF level: 50; mass range (m/z): 70–1050, full MS resolution: 70000; MS/MS resolution: 17500; TopN: 5; NCE/stepped NCE: 20,40.

The data were obtained through experiments. All the measured data were collected by Xcalibur data acquisition software (Thermo, USA), and the qualitative analysis of the compounds corresponding to the chromatographic peaks was completed to screen and determine the chemical components of *P. sibiricum* leaf tea.

2.5. Exploring Active Compounds and Potential Targets in P. sibiricum Leaf Tea: A PubChem and GeneCards Analysis. The PubChem database was used to obtain the molecular structure diagram of the identified compounds. The obtained compounds were introduced into the Swiss ADME platform to screen active compounds. Screening criteria: gastrointestinal absorption (GI absorption) is "high"; two or more of Lipinski, Ghost, Veber, Egan, and Muege results are "yes." Import the screened active compounds into the Swiss target prediction platform to predict the target of active compounds. Only the results with $P > 0.1$ are included, and duplicate targets are deleted to obtain the target information of active compounds. With "Cancer/tumor" as the keyword, query the GeneCards database to obtain candidate targets. Both are standardized through uniport.

2.6. Construction of Protein-Protein Interaction (PPI) Network. The component targets and disease targets were intersected to construct a Venn diagram, and the potential antitumor targets of *P. sibiricum* leaf tea obtained were imported into the STRING database to obtain protein interaction relationships and export relevant data. The color, size, and thickness of nodes and edges are set according to the score value and node degree value by using Cytoscape software, and the protein-protein interaction network diagram is finally obtained.

2.7. Kyoto Encyclopedia of Genes and Genomes (KEGG) Analysis. The potential compound targets of *P. sibiricum* leaf tea for tumor diseases were input into the DAVID database for enrichment analysis of the Kyoto Encyclopedia of Genes and Genomes (KEGG) pathway, with $P < 0.05$ as the screening condition, and the relevant analysis results are obtained.

2.8. Construction of Chemical Compound-Target-Pathway Network (C-T-P) of P. sibiricum Leaf Tea. The chemical component-target-pathway network diagram was constructed by using Cytoscape software. Among them, nodes represent chemical components, targets, and signal pathways, while edges are used to connect chemical components, targets, and signal pathways.

2.9. Molecular Docking Verification of Main Active Components and Core Targets in P. sibiricum Leaf Tea: A Chem 3D, AutoDock, and PyMOL Analysis. Molecular docking verification was carried out for the main active components and core targets of *P. sibiricum* leaf tea. First, optimize the chemical structure of the main active ingredients through Chem 3D, then use AutoDock Tools to determine the information such as the rotatable bonds of ligands, obtain the 3D structure of key targets from the PDB database, and use PyMOL software to remove water, ligands, etc., from proteins. After that, AutoDock 4.26. software was used for hydrogenation and charge calculation of key targets, and we finally use AutoDock Vina software for docking. The results were visualized with PyMOL software.

3. Results

3.1. The Main Chemical Components of P. sibiricum Leaf Tea. The base peak diagram of *P. sibiricum* leaf tea extract was obtained by UPLC-Q-Exactive-MS analysis. The total ion chromatogram (TIC) of ESI-MS in the positive and negative ion modes is shown in Figure 1. According to the molecular weight information of compounds provided by mass spectrometry, 56 compounds were obtained, including 18 compounds in the positive ion mode and 38 compounds in the negative ion mode. Specific compound information is shown in Table 1.

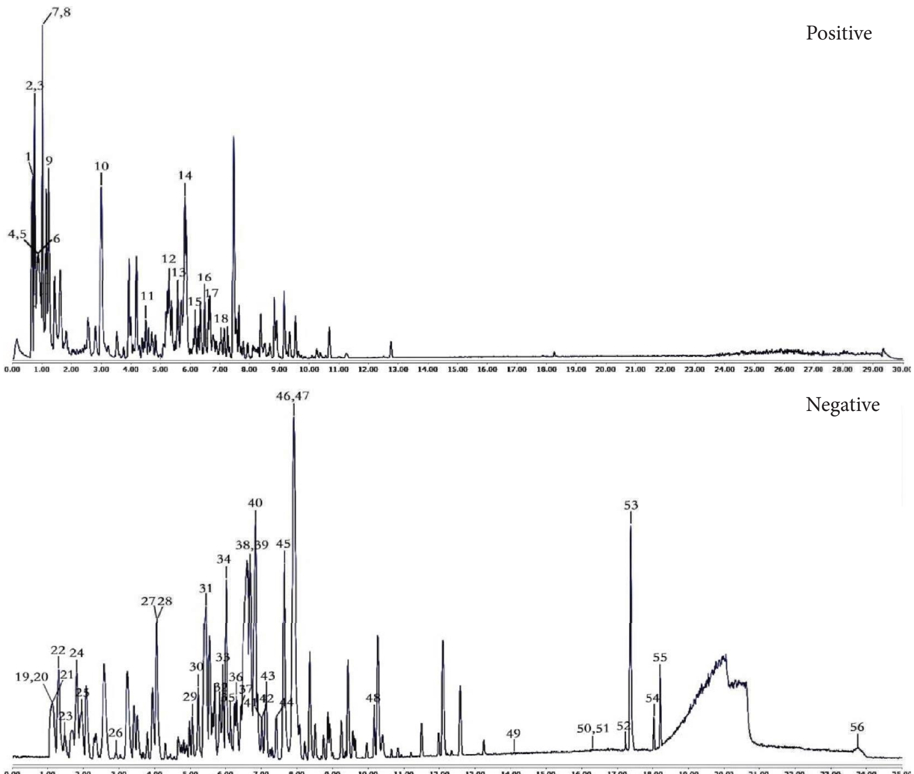

Figure 1: The total ion chromatogram (TIC) of *P. sibiricum* leaf tea in both positive and negative ion modes.

3.2. Target Information of Active Ingredients. Twenty-seven active ingredients were obtained from the chemical components of *P. sibiricum* leaf tea through swissADME screening, and only the results with probability >0.1 were included, corresponding to 373 compound targets. The GeneCards database was used to search for tumor-related targets for disease targets, and 612 disease targets were obtained. A Venn analysis was conducted with Venny 2.1 software to identify common compound targets and disease targets (Figure 2). As a result, 72 targets were determined of the potential targets of *P. sibiricum* leaf tea extract, in terms of its antitumor activity.

3.3. Interactions between Potential Targets of P. sibiricum Leaf Tea. The targets interaction network diagram was obtained using the STRING database and Cytoscape software, as shown in Figure 3. The network graph contains 72 nodes and 578 edges. The size and color depth of nodes are related to the degree value. The larger the degree value, the larger the node, and the larger the combined score, the thicker the edge. In this network, the average degree value of nodes is 16.5, and there are 31 core targets that are greater than the average degree value, as shown in Figure 3. Among them, 11 target proteins have a large degree value (≥ 30), which are AKT1, EGFR, CASP3, CCND1, MTOR, MMP9, ERBB2, BCL2L1, MAPK1, PPARG, and PIK3CA, respectively, indicating that the antitumor effect of *P. sibiricum* leaf tea may be mainly through the above multiple targets.

3.4. Kyoto Encyclopedia of Genes and Genomes (KEGG) Analysis. Screening according to $P < 0.05$, 72 intersection targets were enriched in 130 pathway species, of which 30 pathways were closely related to tumors. Figure 4 shows the results of KEGG pathway analysis of the antitumor effect of *P. sibiricum* leaf tea. The results showed that pathways in cancer, PI3K-Akt signaling pathway and micro-RNAs in cancer, had the highest number of enriched targets, and antitumor related targets such as EGFR were enriched here. This may be the key pathway of the antitumor effect of *P. sibiricum* leaf tea. Therefore, *P. sibiricum* leaf tea plays an antitumor role through the coordination of multiple pathways and may promote apoptosis by participating in the regulation of micro-RNAs, thus inhibiting the proliferation of tumor cells.

3.5. Network Construction and Analysis. The component-target-pathway network diagram was constructed using Cytoscape software, as shown in Figure 5. It can be seen from the figure that the network has 81 nodes, including 8 ingredients, 43 targets, 30 pathways, and 934 edges. The degree values of pubescenol, avenanthamide E, and 13-cis-acitretin, the three key components in Figure 5, are larger than the average value, indicating that they may be the key components of *P. sibiricum* leaf tea to play an antitumor role. Pathways in cancer, PI3K-Akt signaling pathway, and micro-RNAs in cancer have the highest degree values, which may be the potential pathways of the antitumor effect of *P. sibiricum* leaf tea.

Table 1: Chemical composition information of *P. sibiricum* leaf tea.

Peak	Rt (min)	Molecular formula	Theoretical excimer ion peak (m/z)	Measured excimer ion peak (m/z)	Adduct ion	Mass number error (mDa)	Fragment ion	Identified compounds [28–34]
1	0.68	$C_3H_6N_2O_2$	102.0429	103.0502	M + H	1.0073	91.5425; 82.5373	Malonamide
2	0.75	$C_{19}H_{18}O_6$	342.1103	381.0769	M + K	38.9666	219.0256	Mundoserone
3	0.75	$C_4H_9NO_2$	103.0633	104.1070	M + H	1.0437		L(+)-2-aminobutyric acid
4	0.86	$C_9H_{12}N_2$	148.1001	149.1069	M + H	1.0068	130.0858; 102.0549	4-pyrrolidinopyridine
5	0.86	$C_7H_7NO_2$	137.0477	138.0543	M + H	1.0066	110.0599; 94.0420	Trigonelline
6	0.89	$C_5H_9NO_2$	115.0633	116.0702	M + H	1.0069	72.0813	Proline
7	1.01	$C_5H_{11}NO_2$	117.0790	118.0859	M + H	1.0069	102.0551	Dl-norvaline
8	1.01	$C_6H_6N_2O$	122.0480	123.0550	M + H	1.0070	118.0859; 102.0549	Nicotinamide
9	1.23	$C_6H_{13}NO_2$	131.0946	132.1015	M + H	1.0069	116.0705; 86.0967	DL-leucine
10	3.00	$C_9H_{11}NO_2$	165.0790	166.0857	M + H	1.0067	146.0595; 116.0702; 79.0216	Ethyl 4-aminobenzoate
11	4.50	$C_{27}H_{30}O_{15}$	594.1585	595.1625	M + H	1.0040	433.1102; 389.2145;	Vicenin-2
12	5.28	$C_{26}H_{28}O_{14}$	564.1479	565.1535	M + H	1.0056	499.1883; 321.1465	Isoschaftoside
13	5.58	$C_{27}H_{30}O_{16}$	610.1534	611.1559	M + H	1.0025	303.0482; 180.1011; 112.0775	Multinoside A
14	5.81	$C_{21}H_{20}O_{10}$	432.1057	433.1102	M + H	1.0045	326.1787; 195.0645	Isovitexin
15	6.17	$C_{25}H_{26}O_{13}$	534.1373	535.1409	M + H	1.0036	482.2384; 347.1227; 292.1168	5,7-dihydroxy-2-(4-hydroxyphenyl)-6,8-bis(3,4,5-trihydroxyoxan-2-yl) chromen-4-one
16	6.34	$C_{27}H_{31}O_{15}$	595.1663	595.1627	M + H	−0.0036	287.0538; 83.0607	Cyanidin 3-O-rutinoside
17	6.48	$C_{28}H_{32}O_{16}$	624.1690	625.1740	M + H	1.0050	317.0630; 130.1220	Narcissoside
18	7.06	$C_{22}H_{23}O_{11}$	463.1240	463.1203	M + H	−0.0037	301.0681; 287.0899; 127.0386; 83.0671	Peonidin-3-glucoside
19	1.13	$C_9H_8O_4$	180.0423	179.0341	M − H	−1.0082	135.0441	Caffeic acid
20	1.13	$C_9H_6N_2O_3$	190.0378	189.0395	M − H	−0.9983	131.0338; 103.0390	4-nitroquinoline N-oxide
21	1.15	$C_7H_6N_4O_2$	178.0491	177.0397	M − H	−1.0094	131.0338; 116.0705	Melizame
22	1.31	$C_9H_{12}N_2O_6$	244.0695	243.0618	M − H	−1.0077	217.035; 111.0189	Uridine
23	1.48	$C_6H_{13}NO_2$	131.0946	130.0862	M − H	−1.0084	101.0231; 75.0074	L-leucine
24	1.81	$C_{16}H_{18}O_9$	354.0951	353.0881	M − H	−1.0070	191.0552; 176.0394	Chlorogenic acid
25	1.96	$C_{10}H_{13}N_5O_5$	283.0917	282.0843	M − H	−1.0074	225.0402; 195.0296; 156.0654	8-hydroxy-2-deoxyguanosine
26	2.90	$C_7H_6O_2$	122.0368	121.0283	M − H	−1.0085		Benzoic acid
27	4.05	$C_{10}H_{13}N_5O_4$	267.0968	266.0892	M − H	−1.0075	203.0820; 134.0461	Adenosine
28	4.06	$C_{17}H_{15}NO_5$	313.0950	312.0956	M − H	−0.9994	266.0892; 134.0461	Avenanthramide E
29	5.06	$C_{27}H_{30}O_{15}$	594.1585	593.1506	M − H	−1.0079	389.1238; 341.0886; 323.1346	Saponarin
30	5.13	$C_{10}H_{12}N_2O_2$	192.0899	191.0816	M − H	−1.0083	177.0397; 134.0461; 89.0230	N-methyl--oxo-3-pyridinebutanamide
31	5.43	$C_{26}H_{28}O_{14}$	564.1479	563.1400	M − H	−1.0079	449.1668; 281.0870; 134.0601	Isovitexin 2″-O-arabinoside
32	5.82	$C_{21}H_{20}O_{11}$	448.1006	447.0927	M − H	−1.0079	295.0831	2′-hydroxygenistein-8-C-glucoside
33	5.92	$C_{25}H_{26}O_{13}$	534.1373	533.1310	M − H	−1.0063	447.0927; 311.0769	5,7-dihydroxy-2-(4-hydroxyphenyl)-6,8-bis(3,4,5-trihydroxyoxan-2-yl) chromen-4-one
34	6.01	$C_{21}H_{20}O_{10}$	432.1057	431.0984	M − H	−1.0073	197.0704	Vitexin
35	6.07	$C_{27}H_{30}O_{15}$	594.1585	593.1505	M − H	−1.0080	385.0969; 325.1508; 295.0821	8-[4,5-dihydroxy-6-(hydroxymethyl)-3-[3,4,5-trihydroxy-6-(hydroxymethyl)oxan-2-yl]oxyoxan-2-yl]-5,7-dihydroxy-2-(4-hydroxyphenyl)chromen-4-one
36	6.30	$C_{27}H_{31}O_{16}$	611.1612	609.1473	M − 2H	−2.0139	304.0701; 255.2347	Tulipanin
37	6.41	$C_{21}H_{21}O_{12}$	465.1033	463.0876	M − 2H	−2.0157	271.1557; 255.2328	Delphinidin 3-O-glucoside
38	6.71	$C_{26}H_{28}O_{14}$	564.1479	563.1397	M − H	−1.0082	405.2121; 281.0669	6-[(2S,3R,4S,5S,6R)-4,5-dihydroxy-6-(hydroxymethyl)-3-[(2S,3R,4S,5S)-3,4,5-trihydroxyoxan-2-yl]oxyoxan-2-yl]-5,7-dihydroxy-2-(4-hydroxyphenyl)chromen-4-one
39	6.74	$C_{33}H_{40}O_{19}$	740.2164	739.2074	M − H	−1.0090	281.0669; 255.2338; 229.1440	3-[4,5-dihydroxy-3-[(2R,3R,4R,5R,6S)-3,4,5-trihydroxy-6-methyloxan-2-yl]oxy-6-[[(2R,3R,4R,5R,6S)-3,4,5-trihydroxy-6-methyloxan-2-yl] oxymethyl]oxan-2-yl]oxy-5,7-dihydroxy-2-(4-hydroxyphenyl)chromen-4-one
40	6.82	$C_{21}H_{20}O_{10}$	432.1057	431.0985	M − H	−1.0072	297.0896	Homovitexin
41	7.05	$C_5H_5N_5$	135.0545	134.0461	M − H	−1.0107	108.9951	Adenine
42	7.06	$C_{21}H_{20}O_{10}$	432.1057	431.0950	M − H	−1.0084	355.1039; 342.0869; 296.0724; 161.0449	Apigetrin

Table 1: Continued.

Peak	Rt (min)	Molecular formula	Theoretical excimer ion peak (m/z)	Measured excimer ion peak (m/z)	Adduct ion	Mass number error (mDa)	Fragment ion	Identified compounds [28–34]
43	7.10	$C_{27}H_{31}O_{15}$	595.1663	593.1506	M – 2H	−2.0157	431.0984; 342.0883; 255.2348; 134.0460	Cyanidin 3-O-rutinoside
44	7.42	$C_{33}H_{40}O_{20}$	756.2113	755.2017	M – H	−1.0096	349.1523; 255.2338	3-[(2S,4S,6R)-6-[[(2R,3R,4R,5S,6S)-3,5-dihydroxy-6-methyl-4-[(2S,3R,4S,5S,6R)-3,4,5-trihydroxy-6-(hydroxymethyl)oxan-2-yl]oxyoxan-2-yl]oxymethyl]-3,4,5-trihydroxyoxan-2-yl]oxy-5,7-dihydroxy-2-(4-hydroxyphenyl)chromen-4-one
45	7.63	$C_{27}H_{30}O_{15}$	594.1585	593.1506	M – H	−1.0079	431.0984,296.0724	Kaempferol 3-O-β-rutinoside
46	7.90	$C_{23}H_{22}O_{11}$	474.1162	473.1095	M – H	−1.0067	311.0770,236.0508	Germanaism B
47	7.90	$C_{28}H_{32}O_{16}$	624.1690	623.1617	M – H	−1.0073	311.0770; 236.0500	Calendoflavoside
48	10.16	$C_{12}H_{22}O_3$	214.1569	213.1489	M – H	−1.0080	194.9056	4-acetoxy-2-hexyltetrahydrofuran
49	14.16	$C_2H_4O_3$	76.0160	75.0072	M – H	−1.0088		Glycolic acid
50	16.31	CH_4N_2S	76.0095	75.0073	M – H	−1.0022		Thiourea
51	16.31	$C_{14}H_{28}O_2$	228.2089	227.2007	M – H	−1.0082		Myristic acid
52	17.24	$C_{21}H_{26}O_3$	326.1882	325.1841	M – H	−1.0041	183.0115	13-cis-acitretin
53	17.36	$C_{16}H_{32}O_2$	256.2402	255.2328	M – H	−1.0074	92.4210	Palmitic acid
54	18.03	$C_{28}H_{42}O_6$	474.2981	473.2827	M – H	−1.0154	205.1626	Pubescenol
55	18.20	$C_{18}H_{36}O_2$	284.2715	283.2639	M – H	−1.0076		Stearic acid
56	23.79	$C_2H_4O_3$	76.0160	75.0074	M – H	−1.0086		Peracetic acid

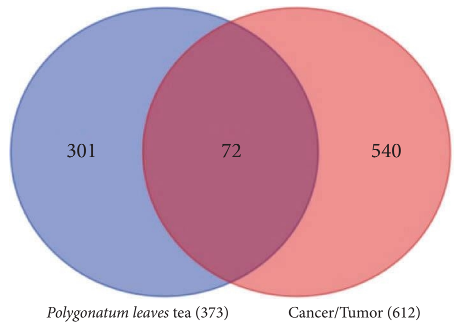

Figure 2: Venn diagram for the antitumor activity of *P. sibiricum* leaf tea.

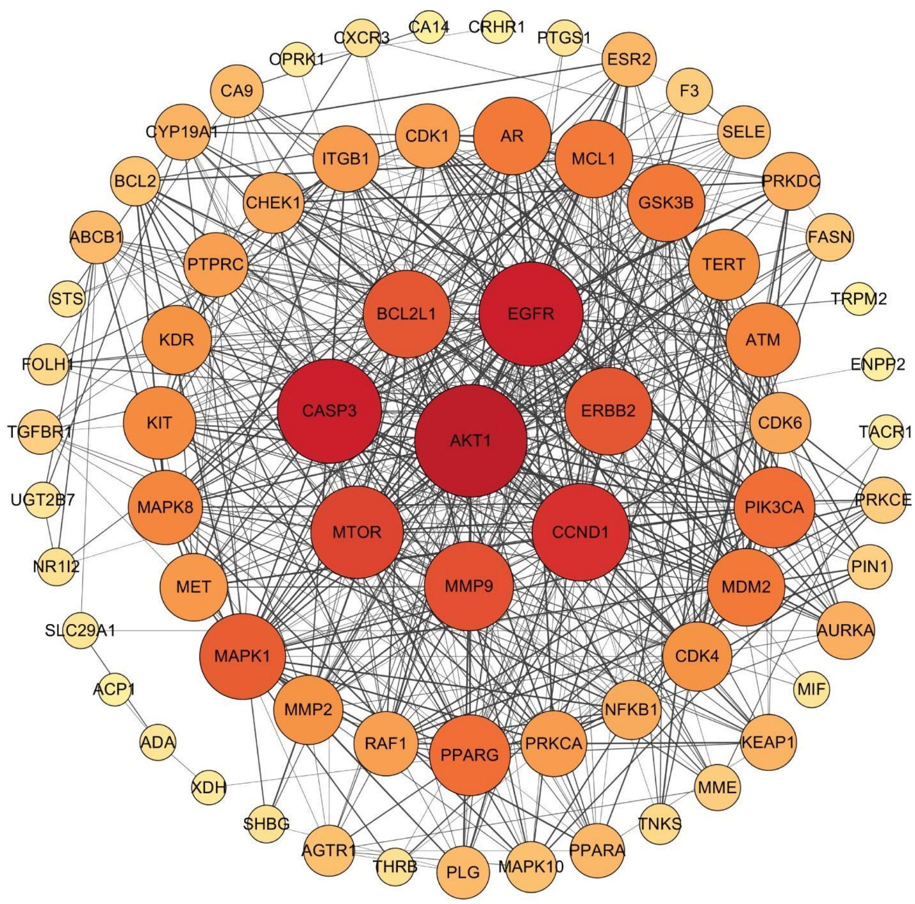

Figure 3: PPI network diagram of intersecting targets.

3.6. Molecular Docking. The three key components are molecularly docked with the first three selected key targets AKT1, EGFR, and CASP3 to judge their binding activity by binding energy. If the binding energy is less than $<-5\,\text{kcal}\cdot\text{mol}^{-1}$, it indicates that they have good binding activity, and if the binding energy is less than $<-7\,\text{kcal}\cdot\text{mol}^{-1}$, it indicates that they have strong binding activity [35]. The results of molecular docking are shown in Table 2 and Figure 6. It can be seen from the results that the binding energies of the three active ingredients and the three core targets are all less than $<-5\,\text{kcal}\cdot\text{mol}^{-1}$, indicating that all compounds can bind well with the targets. The binding energies of pubescenol and 13-cis-acitretin are all less than $<-7\,\text{kcal}\cdot\text{mol}^{-1}$, indicating that they have strong binding activity.

4. Discussion

As can be seen from the C-T-P network diagram, three compounds pubescenol, avenanthramide E, and 13-cis-acitretin had the highest degree values and were much higher than other compounds, so these three compounds were selected as key compounds. Among them, avenanthramide E is an amide compound with antioxidant, anti-inflammatory, and antitumor properties [36]. Guo et al. [37] showed that avenanthramide can significantly inhibit the growth of colon cancer, breast cancer, and prostate cancer cells, especially the proliferation of colon cancer cells. The experiment used avenanthramide to treat human colon adenocarcinoma

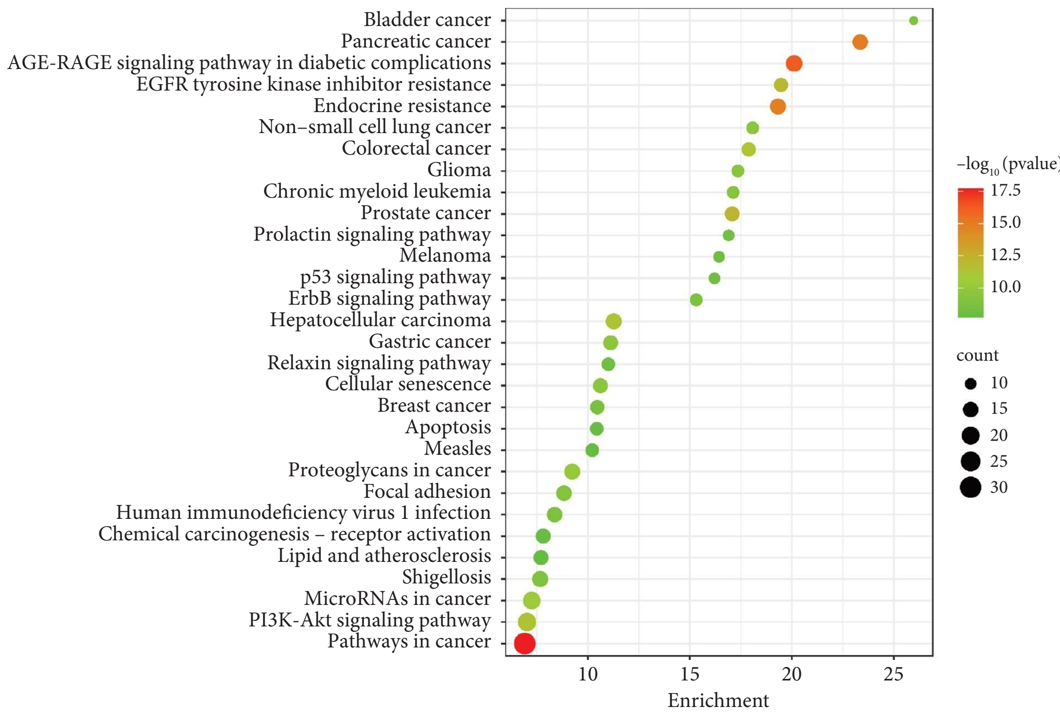

Figure 4: KEGG pathway enrichment analysis results for the antitumor activity of *P. sibiricum* leaf tea.

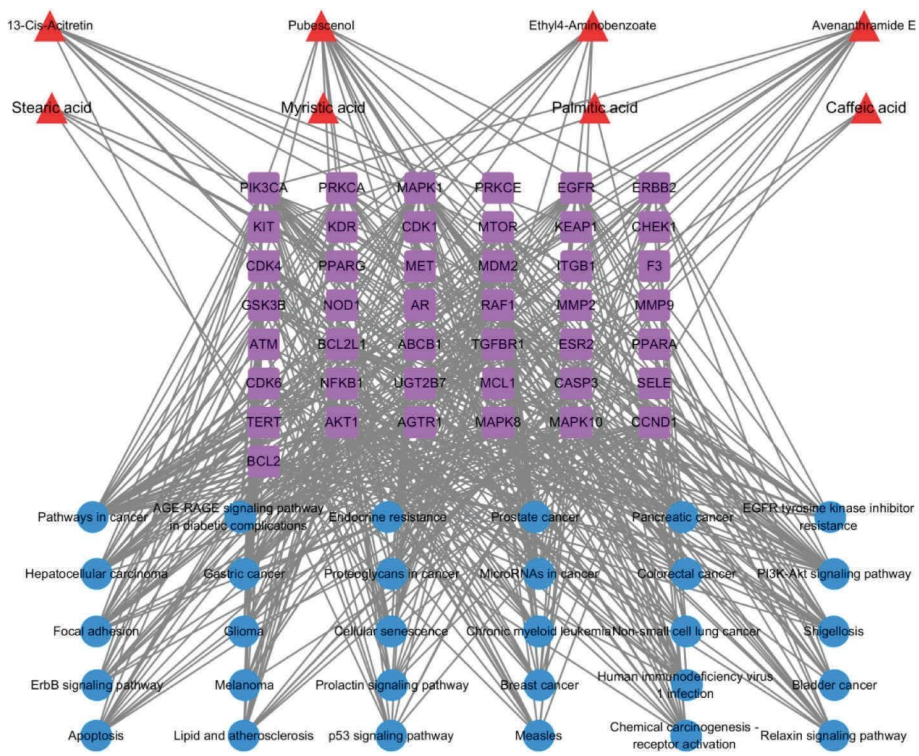

Figure 5: Compound-target-pathway (C–T–P) network for the antitumor activity of *P. sibiricum* leaf tea.

(Caco-2) cells and found that it can effectively inhibit the proliferation of cancer cells in the growth phase. 13-cis-acitretin is an isomer of vitamin A derivatives. It is reported that retinoic acid compounds play an important role in cell proliferation, differentiation, and skin inflammation and have a strong role in inducing differentiation and inhibiting proliferation of tumor cells [38]. Gong [39] showed that combined application of retinoic acid and TNF-α can activate the expression of Caspase-3 protein, increase the expression of Caspase-3, and promote the apoptosis of human epidermal

Table 2: Docking energy results of the complex between key targets and key compounds of *P. sibiricum* leaf tea.

Target	Ingredient		
	Pubescenol	Avenanthramide E	13-cis-acitretin
	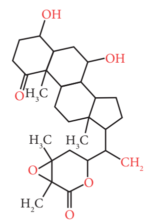	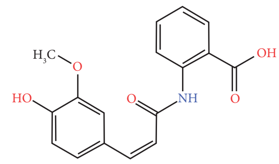	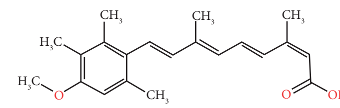
AKT1 (PDBID:6HHG)	−10.54	−6.76	−8.88
EGFR (PDBID:5UG9)	−9.91	−7.42	−8.86
CASP3 (PDBID:2DKO)	−9.49	−6.6	−8.17

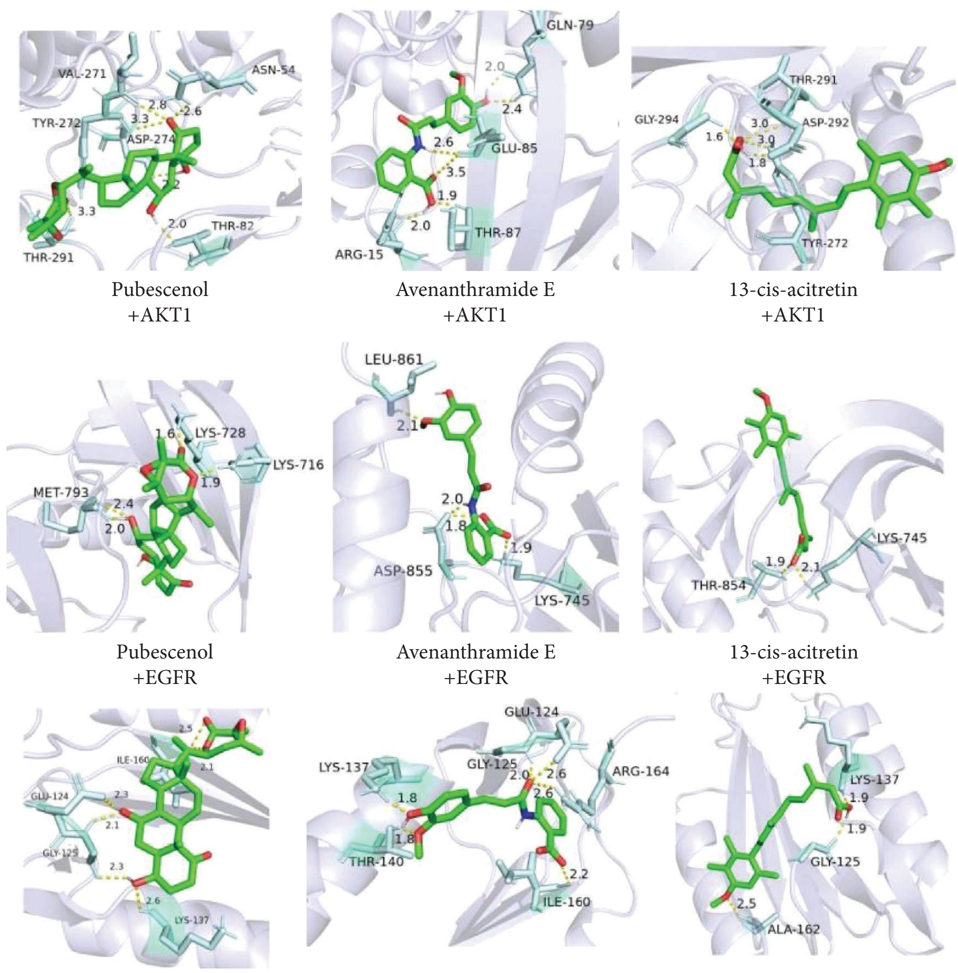

Pubescenol +AKT1; Avenanthramide E +AKT1; 13-cis-acitretin +AKT1

Pubescenol +EGFR; Avenanthramide E +EGFR; 13-cis-acitretin +EGFR

Pubescenol +CASP3; Avenanthramide E +CASP3; 13-cis-acitretin +CASP3

Figure 6: Interaction graphics depicting the relationships between compounds and targets.

squamous cell carcinoma cell A431, which is a feasible way to treat squamous cell carcinoma. Pubescenol is a lactone. Studies have shown that pubescenol is proved to be a moderate inhibitor of the growth of MCF-7, NCI-H460, and SF-268 human tumor cell lines [40].

In this study, 31 core targets, such as AKT1, EGFR, CASP3 and CCND1, were obtained by screening the intersection targets in PPI through the CytoCNA plug-in, and it was predicted that they might be the main antitumor targets of *P. sibiricum* leaf tea. The degree value of AKT1 is the highest among all targets. It is a silk/threonine protein kinase, which can regulate cell proliferation and growth, and plays an important role in the regulation of cell apoptosis and cell cycle [41]. CASP3 is mainly involved in the apoptosis process of cells. Whether the exogenous signal pathway or the endogenous signal pathway, CASP3 must be activated to convert into the activated form of C-CASP3 in order to carry out the final apoptosis process of cells. Induction of apoptosis is a common pathway of many chemotherapeutic drugs and targeted therapeutic drugs [42, 43]. EGFR is the expression product of proto-oncogene c-erb-B1, which is highly/abnormally expressed in many solid tumors and is related to the growth, proliferation, differentiation, and apoptosis of tumor cells [44, 45].

The enrichment analysis results of the KEGG pathway show that the three pathways, pathways in cancer, PI3K-Akt signaling pathway, and micro-RNAs in cancer, have the highest enrichment. The PI3K-Akt signaling pathway is a classic cancer signal pathway. As an important intracellular signal transduction pathway, the PI3K-Akt signaling pathway plays an important role in cell proliferation and apoptosis, and its overactivation is closely related to tumor genesis and development. Activated Akt can directly phosphorylate forkhead transcription factor (FoxO) family, promote its binding with antiapoptosis binding protein, and thus inhibit cell apoptosis. In addition, this signal pathway can also promote tumor cell proliferation and metastasis by up regulating the expression of matrix metalloproteinase-2 mRNA and regulate tumor tissue angiogenesis by promoting tumor necrosis factor (TNF)-induced endothelial cell migration [46]. Therefore, inhibiting the expression of this signal pathway is conducive to preventing the proliferation and proliferation of tumor cells and promoting tumor cell apoptosis.

It is worth noting that Huang et al. previously conducted a study on the network pharmacological antitumor activity of *P. sibiricum* flower [33]. We acknowledge that *P. sibiricum* leaves possess abundant resources, and if they can be utilized to create a health-promoting tea, it would hold a significant value. However, our study specifically focuses on analyzing the components of *P. sibiricum* leaf tea and their potential in targeting and affecting tumor growth pathways. Regarding our methods and analytical techniques, our manuscript primarily utilizes UPLC-Q-Exactive-MS for metabolite profiling and identification. This technique offers several advantages over UPLC-Q-TOF-MSE, including enhanced mass resolution and accuracy, improved sensitivity, expanded dynamic range, high mass accuracy for structural elucidation, comprehensive metabolite profiling, database searching capabilities, and faster analysis time.

5. Conclusions

In this study, UPLC-Q-Exactive-MS was used to qualitatively analyze the chemical components of *P. sibiricum* leaf tea. From this, we identified 56 chemical components, and then we used network pharmacology for target recognition, path analysis, and network construction. To the best of our knowledge, this method has been used for the first time to explain the efficacy and the material basis of the molecular mechanism of the antitumor effect of the *P. sibiricum* leaf tea. Three key compounds and eleven key targets were obtained by constructing a component target pathway network diagram, and 30 antitumor related pathways were identified by KEGG pathway analysis. The docking results of three key compounds were basically consistent with the results of network pharmacology. This study reflects the action characteristics of *P. sibiricum* leaf tea extract with multiple components, multiple targets, and multiple pathways and identifies the antitumor active components of *P. sibiricum* leaf tea and its potential mechanism of action, which can provide clues and inspiration for the follow-up research on new mechanisms of action.

Data Availability

The data used to support the findings of this study are included in the article.

Conflicts of Interest

The authors declare that they have no conflicts of interest.

Authors' Contributions

Xiaodan Zhang, Ruilian Han, and Zhongda Zeng designed and guided all the experiments and rewrote and revised the manuscript. Jie Chen analyzed the data and wrote the preliminary manuscript. Jie Xia, Feng Yin, and Jiani Yu analyzed the corresponding data and double checked the data. Jinfeng Huo and Yingjiao Shi conducted the chemical experiments. All authors have read and approved the final manuscript.

Acknowledgments

The authors gratefully acknowledge the financial support from the Key Research and Development Project of Zhejiang Province (2020C02039) and the Major Science and Technology Projects of Breeding New Varieties of Agriculture in Zhejiang Province (no. 2021C02074).

References

[1] S. Liu, Q. J. Jia, Y. Q. Peng, T. H. Feng, S. T. Hu, and Z. S. Liang, "Advances in mechanism research on *Polygonatum* in prevention and treatment of diabetes," *Frontiers in Pharmacology*, vol. 13, Article ID 758501, 2022.

[2] H. Jiang, "The study of anti-tumour activity of *rhizoma Polygonati*," *Journal of Nanjing Tcm University*, vol. 26, no. 6, pp. 479-480, 2010.

[3] K. D. K. Wenceslas, N. K. Frédéric, K. K. Léandre, and Y. A. Paul, "Anti-inflammatory effects of an aqueous extract of justicia flava (forsk) vahl (acanthaceae) in rats," *Asian Journal of Pharmaceutical and Clinical Research*, vol. 14, pp. 146–153, 2021.

[4] Y. Chen and X. S. Sun, "Advances in pharmacological research of *Polygonati rhizoma*," *Traditional Chinese Drug Research and Clinical Pharmacology*, vol. 21, no. 3, pp. 328–330, 2010.

[5] T. H. Feng, Q. J. Jia, X. Meng et al., "Evaluation of genetic diversity and construction of DNA fingerprinting in *Polygonatum* Mill. based on EST-SSR and SRAP molecular markers," *3 Biotech*, vol. 10, no. 7, Article ID 322, 2020.

[6] T. H. Feng, Y. J. Jiang, Q. J. Jia et al., "Transcriptome analysis of different sections of rhizome in *Polygonatum sibiricum* red. And mining putative genes participate in polysaccharide biosynthesis," *Biochemical Genetics*, vol. 60, no. 5, pp. 1547–1566, 2022.

[7] Q. W. Yang, Y. J. Jiang, Y. P. Wang et al., "SSR loci analysis in transcriptome and molecular marker development in *Polygonatum sibiricum*," *BioMed Research International*, vol. 2022, Article ID 4237913, 9 pages, 2022.

[8] F. F. Wang, Y. J. Jiang, S. F. Jin et al., "Structure characterization and bioactivity of neutral polysaccharides from different sources of *Polygonatum* Mill," *Biopolymers*, vol. 113, no. 6, Article ID e23490, 2022.

[9] Y. F. Wang, Z. X. Zhang, and R. J. He, "Study on the chemical constituents of the aerial parts of Polygonatum sibiricum and its pancreatic lipase inhibitory activity," *Natural Product Research and Development*, vol. 32, pp. 1811–1817, 2020.

[10] F. Bray, J. Ferlay, I. Soerjomataram, R. L. Siegel, L. A. Torre, and A. Jemal, "Global cancer statistics 2018: GLOBOCAN estimates of incidence and mortality worldwide for 36 cancers in 185 countries," *CA-A Cancer Journal for Clinicians*, vol. 68, no. 6, pp. 394–424, 2018.

[11] L. Zhang, M. Wang, and X. X. Zhang, "The mechanism of chelerythrine against breast cancer by network pharmacology and molecular docking," *Journal of Xi'an Jiaotong University*, vol. 42, no. 4, pp. 554–561, 2021.

[12] W. Y. Hu, Y. J. Zheng, P. G. Xia, and Z. Liang, "The research progresses and future prospects of Tetrastigma hemsleyanum Diels et Gilg: a valuable Chinese herbal medicine," *Journal of Ethnopharmacology*, vol. 271, Article ID 113836, 2021.

[13] L. Li, X. Zhou, and X. J. Gong, "Progress of research on the antiendometrial cancer effects and mechanisms oftraditional Chinese medicine and natural product," *Natural Product Research and Development*, vol. 33, pp. 2146–2156, 2021.

[14] J. N. Yu, J. Xia, J. X. Xu et al., "Chemical profile, antihepatoma activity, anti-acetylcholinesterase and antioxidant activity of aerial part of *Aconitum carmichaeli* Debx," *Natural Product Research*, vol. 37, no. 22, pp. 3884–3888, 2022.

[15] P. Wang, S. Q. Yang, M. Qasim, and A Thu Phyo, "Jatrorrhizine inhibits colorectal carcinoma proliferation and metastasis through Wnt/β-catenin signaling pathway and epithelial-mesenchymal transition," *Drug Design, Development and Therapy*, vol. 13, pp. 2235–2247, 2019.

[16] J. Xia, X. Y. Li, M. Lin et al., "Screening out biomarkers of *Tetrastigma hemsleyanum* for anti-cancer and anti-inflammatory based on spectrum-effect relationship coupled with UPLC-Q-TOF-MS," *Molecules*, vol. 28, no. 7, p. 3021, 2023.

[17] X. D. Zhang, Y. S. Cen, Y. G. Yu et al., "Simultaneous determination of 17 constituents of Chinese wild radix salvia miltiorrhiza from different geographical areas by ultra-high performance liquid chromatography coupled to triple quadrupole mass spectrometry," *Current Pharmaceutical Analysis*, vol. 16, no. 3, pp. 280–290, 2020.

[18] Y. Liang, L. Li, Y. Cai et al., "Analysis of chemical constituents in ethyl acetate extract of Taxilli Herba by UPLC-Q-Exactive-MS and screening of potential xanthine oxidase inhibitors," *China Journal of Chinese Materia Medica*, vol. 47, no. 4, pp. 972–979, 2022.

[19] K. Ren, R. J. Wang, S. N. Fang et al., "Effect of CYP3A inducer/inhibitor and licorice on hepatotoxicity and in vivo metabolism of main alkaloids of Euodiae Fructus based on UPLC-Q-Exactive-MS," *Journal of Ethnopharmacology*, vol. 303, Article ID 116005, 2023.

[20] J. Liu, Z. Y. Hu, A. R. Zheng, Q. Ma, and D. Liu, "Identification of exudate metabolites associated with quality in beef during refrigeration," *LWT-Food Science and Technology*, vol. 172, Article ID 114241, 2022.

[21] Z. H. Li and G. Q. Zhang, "Metabolomic analysis reveals the quality characteristics of Yi Gong tea leaves at different harvesting periods," *Journal of Food Biochemistry*, vol. 46, no. 12, pp. 144788–e14511, 2022.

[22] G. H. Jian, B. Z. Su, W. J. Zhou, and H. Xiong, "Application of network pharmacology and molecular docking to elucidatethe potential mechanism of *Eucommia ulmoides-Radix Achyranthis Bidentatae* against osteoarthritis," *BioData Mining*, vol. 13, no. 1, pp. 12–18, 2020.

[23] Z. Y. Wang, X. Wang, D. Y. Zhang, Y. J. Hu, and S. Li, "Traditional Chinese medicine network pharmacology: development in new era under guidance of network pharmacology evaluation method guidance," *China Journal of Chinese Materia Medica*, vol. 47, no. 1, pp. 7–17, 2022.

[24] X. Jie, Y. Feng, F. Jiahao et al., "Comprehensive chemical profiling of two Dendrobium species and identification of antihepatoma active constituents from Dendrobium chrysotoxum by network pharmacology," *Bone Marrow Concentrate Complementary Medicine and Therapies*, vol. 23, no. 1, p. 217, 2023.

[25] S. H. Zheng, T. Y. Xue, B. Wang, H. Guo, and Q. Liu, "Application of network pharmacology in the study of mechanism of Chinese medicine in the treatment of ulcerative colitis: a review," *Frontiers in Bioinformatics*, vol. 2, Article ID 928116, 2022.

[26] Y. C. Peng, R. Tang, L. Y. Ding et al., "Diosgenin inhibits prostate cancer progression by inducing UHRF1 protein degradation," *European Journal of Pharmacology*, vol. 942, Article ID 175522, 2023.

[27] W. C. Xiong, H. Z. Wu, Y. Y. Xiong, B. Liu, S. Wu, and Y. Yang, "Network pharmacology-based research of active components of albiziae flos and mechanisms of its antidepressant effect," *Current Medical Science*, vol. 40, no. 1, pp. 123–129, 2020.

[28] B. Yang, J. Y. Huang, and S. J. Zheng, "Component analysis of *Polygonatum sibiricum, Polygonatum cyrtonema* and *Polygonatum kingianum* based on UPLC-Q/TOF-MS technology," *Acta Chinese Medicine and Pharmacology*, vol. 50, no. 10, pp. 43–51, 2022.

[29] K. Y. Ji, H. P. Wang, and J. Yang, "Rapid analysis and identification of the chemical constituents of wild *Polygonatum kingianum* Coll.et Hemsl in Sichuan Aba by UPLC-Q-TOF-MS^E," *Applied Chemical Industry*, vol. 48, no. 1, pp. 271–275, 2019.

[30] D. D. Cheng, C. N. Li, and J. W. Lv, "Rapid screening of active ingredient that inhibiting angiotensin-converting enzyme in *Polygonati Rhizoma* by LC-MS/MS with molecular docking technology," *Modern Food Science and Technology*, vol. 39, no. 5, pp. 1–9, 2023.

[31] Y. M. Yu, X. Y. Ma, and T. J. Zhang, "Rapid characterization on components of *Polygonatum sibiricum* based on HPLC-MS technology," *Lishizhen Medicine and Materia Medica Research*, vol. 27, no. 4, pp. 794–796, 2016.

[32] Z. Z. Huang, X. Du, C. D. Ma, R. Zhang, W. Gong, and F. Liu, "Identification of antitumor active constituents in *Polygonatum sibiricum* flower by UPLC-Q-TOF-MS^E and network pharmacology," *American Chemical Society Omega*, vol. 5, no. 46, pp. 29755–29764, 2020.

[33] Z. Y. Sui, P. Y. Hou, and B. Wang, "Rapid identification of the components in *Polygonatum ordoratum* based on UPLC-Q-Orbitrap platform," *China Pharmacy*, vol. 25, no. 4, pp. 626–630, 2022.
[34] H. Y. Wang, L. Li, and Y. J. Dong, "Analysis of chemical constituents of *Polygonatum ordoratum* based on UPLC-Q-TOF/MS technique," *Journal of China Prescription Drug*, vol. 16, no. 9, pp. 37-38, 2018.
[35] J. L. Cai, X. P. Li, Y. L. Zhu et al., "Mechanism of Huangjing Qianshi Decoction in treatment of prediabetes based on network pharmacology and molecular docking," *China Journal of Chinese Materia Medica*, vol. 47, no. 4, pp. 1039–1050, 2022.
[36] Y. H. Yu, L. Y. Zhou, X. P. Li et al., "The progress of nomenclature, structure, metabolism, and bioactivities of oat novel phytochemical: avenanthramides," *Journal of Agricultural and Food Chemistry*, vol. 70, no. 2, pp. 446–457, 2022.
[37] W. Guo, L. Nie, D. Wu et al., "Avenanthramides inhibit proliferation of human colon cancercell lines in vitro," *Nutrition and Cancer*, vol. 62, no. 8, pp. 1007–1016, 2010.
[38] Q. Fan, X. H. Su, and W. X. Wang, "Redifferentiation therapy with 13-cis retinoid acid in differentiated thyroid carcinoma," *Progress in Modern Biomedicine*, vol. 15, no. 34, pp. 6659–6663, 2015.
[39] M. J. Gong, *The Effect of Acitretin Combined TNF-α on Human Cutaneous Squamous Carcinoma A431 Cells and its Mechanism*, Hebei Medical University, Shijiazhuang, China, 2012.
[40] C. Valente, M. Pedro, A. Duarte, M. S. J. Nascimento, P. M. Abreu, and M. J. U. Ferreira, "Bioactive diterpenoids, a new jatrophane and two ent-abietanes, and other constituents from Euphorbia pubescens," *Journal of Natural Products*, vol. 67, no. 5, pp. 902–904, 2004.
[41] S. E. Degan and I. H. Gelman, "Emerging roles for AKT isoform preference in cancer progression pathways," *Molecular Cancer Research*, vol. 19, no. 8, pp. 1251–1257, 2021.
[42] Y. Yuan, Z. L. Ding, J. C. Qian et al., "Casp3/7-instructed intracellular aggregation of Fe3O4 nanoparticles enhances T2 MR imaging of tumor apoptosis," *Nano Letters*, vol. 16, no. 4, pp. 2686–2691, 2016.
[43] J. Q. Huang, H. L. Liang, and X. C. Zhang, "Expression and significance of CASP3 and C-CASP3 in lung cancer," *The Journal of Practical Medicine*, vol. 28, no. 8, pp. 1247–1250, 2012.
[44] F. F. Chen, L. Zhang, J. Q. Wu et al., "HCRP-1 regulates EGFR-AKT-BIM-mediated anoikis resistance and serves as a prognostic marker in human colon cancer," *Cell Death and Disease*, vol. 9, no. 12, pp. 1176–1190, 2018.
[45] M. Ghothim, J. Srovnal, L. Bébarová et al., "Determination of CEA, EGFR and hTERT expression in peritoneallavage in patients with pancreatic adenocarcinoma using RT-PCR method," *Rozhledy v Chirurgii: Měsíčník Československé Chirurgické Společnosti*, vol. 94, no. 11, pp. 464–469, 2015.
[46] A. C. Colmone, F. Sallusto, and A. K. Abbas, "Promoting immunology: the future is here," *Science Immunology*, vol. 1, no. 1, p. 2713, 2016.